A journal for the publication of
original research in all branches of physics

www.publish.csiro.au/journals/ajp

CSIRO
AUSTRALIA

Academy of Science

Elastic Scattering of Low-energy Electrons by OCS Molecules

M. H. F. Bettega,[A] *M. A. P. Lima*[B] *and L. G. Ferreira*[B]

[A] Departamento de Física, Universidade Federal do Paraná,
Caixa Postal 19081, 81531–990, Curitiba, Paraná, Brazil.
[B] Instituto de Física 'Gleb Wataghin', Universidade Estadual de Campinas,
Caixa Postal 6165, 13083–970, Campinas, São Paulo, Brazil.

Abstract

We report results from an *ab initio* calculation of low-energy electron scattering by OCS molecules. We used the Schwinger multichannel method with pseudopotentials at the fixed-nuclei static-exchange approximation to calculate elastic integral, differential and momentum transfer cross sections in the energy range from 5 to 50 eV. We compare our results with available theoretical results and experimental data. Through the symmetry decomposition of our integral cross section and eigenphase sum analysis, we found structures in the cross sections that may be interpreted as shape resonances for Σ, Π and Δ symmetries. We compared the results for OCS with our previous results on the e^-–CS_2 collision. In particular, we found a similar behaviour in the shape of the symmetry decomposed cross sections of OCS and of CS_2 when, for the latter, we sum over the 'g' and 'u' contributions.

1. Introduction

Studies on electron collisions with OCS molecules have received some attention in past years. We can quote the theoretical work of Lynch and Dill (1979), measurements of the total cross section by Szmytkowski *et al.* (1984), measurements of the elastic cross sections by Sohn *et al.* (1987) and the more recent work by Raj and Tomar (1989) and by Sakamoto *et al.* (1999). Lynch and Dill (1979) used the continuum multiple-scattering model and studied elastic e^-–OCS scattering from 0 to 100 eV. They were able to find some shape resonances, especially the low-energy Π shape-resonance around $1 \cdot 85$ eV. The measurements of Sohn *et al.* (1987) covered the energy range from $0 \cdot 3$ to 5 eV. Szmytkowski *et al.* measured total cross sections covering the energy range from $0 \cdot 4$ to 80 eV, while Raj and Tomar (1989) applied the independent atom model to calculate the cross section for energies above 100 eV. Sakamoto *et al.* (1999) measured the elastic differential cross sections at 2, 8, 15 and 100 eV. To our knowledge, there are no results for either the differential cross section or momentum transfer cross sections in the energy range from 5 to 50 eV for OCS molecules, except for the results of Sohn *et al.* (1987) at 5 eV and of Sakamoto *et al.* (1999) at 8 and 15 eV.

In this work we present results of calculations on the elastic e^-–OCS collision obtained with the Schwinger multichannel (SMC) method with pseudopotentials (SMCPP) (Bettega *et al.* 1993) at the fixed-nuclei static-exchange approximation. We consider energies ranging from 5 to 50 eV, thus avoiding the low-energy range

where polarisation effects are known to be important in giving a correct description of the scattering process. In order to describe the long range interaction due to the permanent dipole moment of OCS, and therefore to improve the behaviour of the differential cross sections at small scattering angles, we include in our calculation the dipole moment potential through the first Born approximation (FBA) (Varella *et al.* 1999). We investigate the symmetry decomposition of the integral cross section and the eigenphase sum in order to look for a resonant behaviour for some of the symmetries of OCS. We also make a comparison between our cross sections for OCS with our previous CS_2 results (Bettega *et al.* 1999). OCS and CS_2 have the same number of valence electrons, and both are linear and made of equivalent atoms. Thus, a comparison between their cross sections would be interesting, especially when the CS_2 cross sections are summed over the the 'g' and 'u' contributions that would reflect the loss of one symmetry plane (perpendicular to the molecular axis) by CS_2.

In the next sections we present the theoretical formulation of our method, our computational procedures, the results and a discussion. We end this work with a brief summary.

2. Theoretical Formulation

Here we give a brief description of the SMC (Takatsuka and McKoy 1981; Takatsuka and McKoy 1984; Lima *et al.* 1990) and SMCPP (Bettega *et al.* 1993) methods. The SMC method is a multichannel extension of the Schwinger variational principle. Actually, it is a variational approximation for the scattering amplitude, where the scattering wave function is expanded in a basis of $(N + 1)$-particle Slater determinants:

$$|\Psi_{\vec{k}}\rangle = \sum_m a_m^\pm(\vec{k})|\chi_m\rangle \,, \tag{1}$$

and the coefficients $a_m^\pm(\vec{k})$ of this expansion are then variationally determined. The resulting expression for the scattering amplitude in the body frame, a reference frame attached to the molecule in order to take advantage of its symmetries, is

$$[f_{\vec{k}_i,\vec{k}_f}] = -\frac{1}{2\pi} \sum_{m,n} \langle S_{\vec{k}_f}|V|\chi_m\rangle (d^{-1})_{mn} \langle \chi_n|V|S_{\vec{k}_i}\rangle \,, \tag{2}$$

where

$$d_{mn} = \langle \chi_m|A^{(+)}|\chi_n\rangle \,, \tag{3}$$

$$A^{(+)} = \frac{\hat{H}}{N+1} - \frac{(\hat{H}P + P\hat{H})}{2} + \frac{(VP + PV)}{2} - VG_P^{(+)}V \,. \tag{4}$$

In the above equations $|S_{\vec{k}_i}\rangle$, the solution of the unperturbed Hamiltonian H_0, is the product of a target state and a plane wave, V is the interaction potential between the incident electron and the target, $|\chi_m\rangle$ is an $(N + 1)$-electron Slater determinant used in the expansion of the trial scattering wave function, $\hat{H} = E - H$

is the total energy of the collision minus the full Hamiltonian of the system, with $H = H_0 + V$, P is a projection operator onto the open-channel space defined by target eigenfunctions $|\Phi_l\rangle$,

$$P = \sum_{l}^{\text{open}} |\Phi_l\rangle\langle\Phi_l|, \tag{5}$$

and $G_P^{(+)}$ is the free-particle Green function projected on the P-space.

For elastic scattering at the static-exchange approximation, the P operator is composed only of the ground state of the target $|\Phi_1\rangle$

$$P = |\Phi_1\rangle\langle\Phi_1|, \tag{6}$$

and the configuration space $|\chi_m\rangle$ is

$$\{|\chi_m\rangle\} = \{\mathcal{A}|\Phi_1\rangle|\varphi_m\rangle\}, \tag{7}$$

where $|\varphi_m\rangle$ is a one-particle function represented by one molecular orbital. This molecular orbital, usually a canonical virtual orbital obtained in a Hartree–Fock calculation, is used to represent the continuum electron. This choice is justified by the fact that in the SMC method the scattering wave function has to be well described only within the range of the potential (Takatsuka and McKoy 1981, 1984). In general, the interaction potential is short-ranged and the SMC method gives a good description of the scattering wave function.

With the choice of Cartesian Gaussian functions to represent the molecular and scattering orbitals, all the matrix elements arising in equation (2) can be computed analytically, except those from $\langle\chi_m|VG_P^{(+)}V|\chi_n\rangle$ (VGV) which are evaluated by numerical quadrature (Lima *et al.* 1990).

The numerical calculation of the matrix elements from VGV is the most intensive step in the SMC code and demands almost the entire computational time of the scattering calculation. These matrix elements are reduced to a sum of primitive two-electron integrals involving a plane wave and three Cartesian Gaussians:

$$\langle\alpha\beta|V|\gamma\vec{k}\rangle = \int\int d\vec{r}_1\, d\vec{r}_2\,\alpha(\vec{r}_1)\beta(\vec{r}_1)\,\frac{1}{r_{12}}\,\gamma(\vec{r}_2)e^{i\vec{k}.\vec{r}_2}, \tag{8}$$

and must be evaluated for all possible combinations of α, β and γ and for several directions and moduli of $\vec{k}$. We must also evaluate the one-electron integrals of the type

$$\langle\alpha|V^{\text{PP}}|\vec{k}\rangle = \int d\vec{r}\,\alpha(\vec{r})V^{\text{PP}}e^{i\vec{k}.\vec{r}}. \tag{9}$$

These one-electron integrals are more complex than those involving the nuclei, but they can be calculated analytically and their number is also reduced due to the smaller basis set. In the above equation, V^{PP} is the nonlocal pseudopotential

operator given by

$$\hat{V}^{\mathrm{PP}}(r) = \hat{V}_{\mathrm{core}}(r) + \hat{V}_{\mathrm{ion}}(r)\,, \tag{10}$$

with

$$\hat{V}_{\mathrm{core}}(r) = -\frac{Z_v}{r}\left[\sum_{i=1}^{2} c_i^{\mathrm{core}}\mathrm{erf}\left[(\alpha_i^{\mathrm{core}})^{\frac{1}{2}}\,r\right]\right]\,, \tag{11}$$

$$\hat{V}_{\mathrm{ion}}(r) = \sum_{n=0}^{1}\sum_{j=1}^{3}\sum_{l=0}^{2} A_{njl}r^{2n}e^{-\alpha_{jl}r^2}\sum_{m=-l}^{+l}|lm\rangle\langle lm|\,. \tag{12}$$

Here Z_v is the valence charge of the atom and in this application is equal to 4 for C and 6 for O and S. The coefficients c_i^{core}, A_{njl} and the decay constants α_i^{core} and α_{jl} are tabulated in the work of Bachelet *et al.* (1982).

Even for small molecules, a large number of two-electron integrals must be evaluated. This limits the size of molecules in scattering calculations. In the SMCPP method we need a shorter basis set to describe the target and scattering and consequently the number of two electron integrals is smaller than in the all-electron case. The reduction in the number of these integrals allows the study of molecules larger than those reached by all-electron techniques.

The Born closure procedure is discussed elsewhere (Varella *et al.* 1999) for the dipole-allowed rotational excitation $00 \rightarrow 10$ of a symmetric top, and we believe that its extension to the elastic scattering case is a trivial matter. Therefore we present only the final expression, given by

$$f_{\vec{k}_i,\vec{k}_f} = f^{\mathrm{FBA}}(\vec{k}_i,\vec{k}_f) \;+\; \sum_{l=0}^{l_1}\sum_{m=-l}^{+l}\left[a_{lm}^{\mathrm{SMCPP}}(\hat{k}_i,k_f) - a_{lm}^{\mathrm{FBA}}(\hat{k}_i,k_f)\right]Y_{lm}(\hat{k}_f)\,, \tag{13}$$

where

$$f^{\mathrm{FBA}}(\vec{k}_i,\vec{k}_f) = 2i\frac{\vec{D}\cdot(\vec{k}_i - \vec{k}_f)}{|\vec{k}_i - \vec{k}_f|^2} \tag{14}$$

is the dipole moment potential expression for the scattering amplitude in the first Born approximation; a_{lm}^{SMCPP} and a_{lm}^{FBA} are, respectively, the coefficients of expansion of equations (2) and (14) in the spherical harmonics Y_{lm}. In equation (14), $\vec{D}$ is the permanent dipole moment of the target; $\hat{k}_i$ and $\hat{k}_f$ are, respectively, the incident and outgoing directions in the laboratory frame of reference. Details about the relation between the incident direction and the Eulerian angles that define the transformation from the molecular frame to the laboratory frame, and also about the Fourier transform of the pseudopotentials, are discussed by Varella *et al.* (1999).
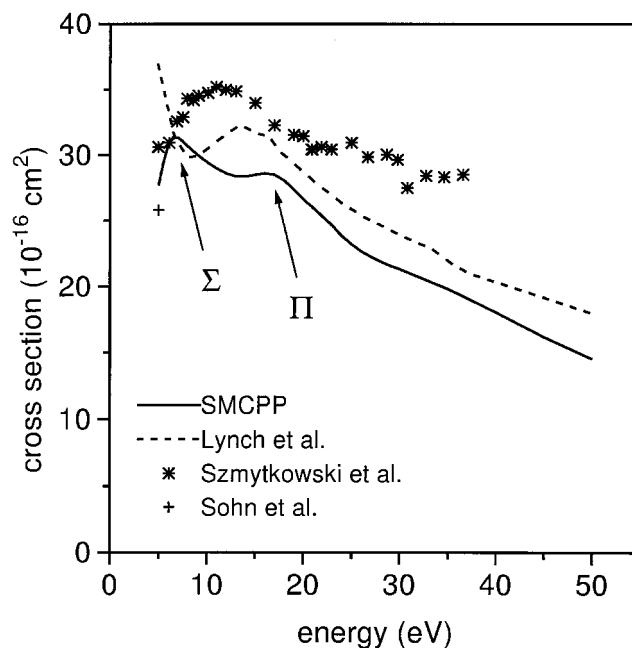
3. Computational Procedures

The ground state of the molecule $^1\Sigma$ is described by a single-configuration wave function $|\Phi_1\rangle$ (Hartree–Fock level) at the experimental geometry with

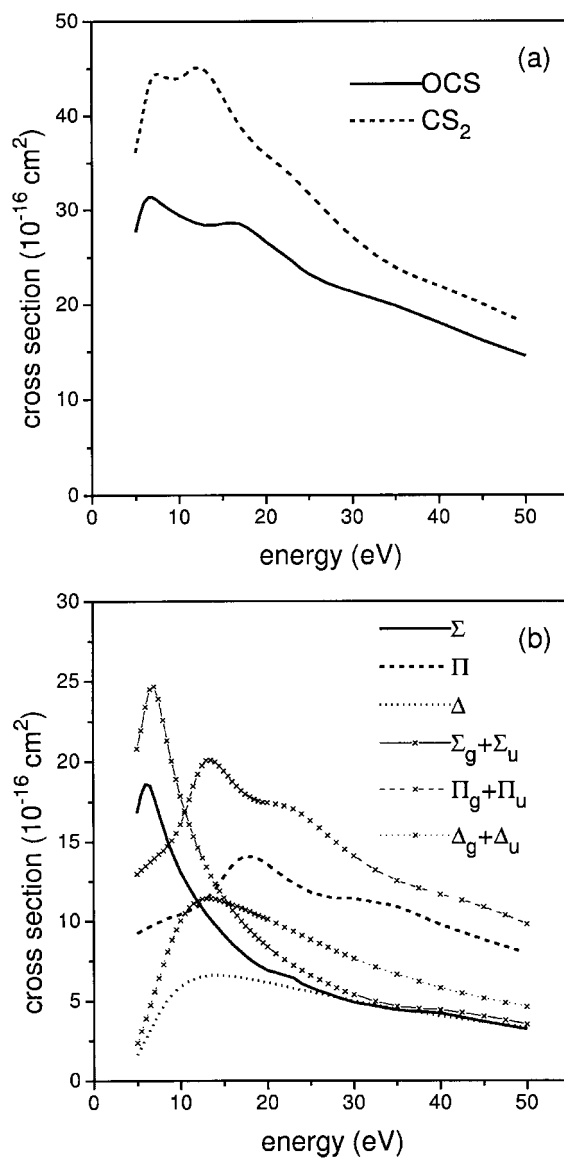**Table 1.   Cartesian Gaussian functions for oxygen, carbon and sulfur**

Cartesian Gaussian functions are defined by
$$\phi_{lmn} = N_{lmn}(x - a_x)^l(y - a_y)^m(z - a_z)^n \exp(-\alpha|\vec{r} - \vec{a}|^2)$$

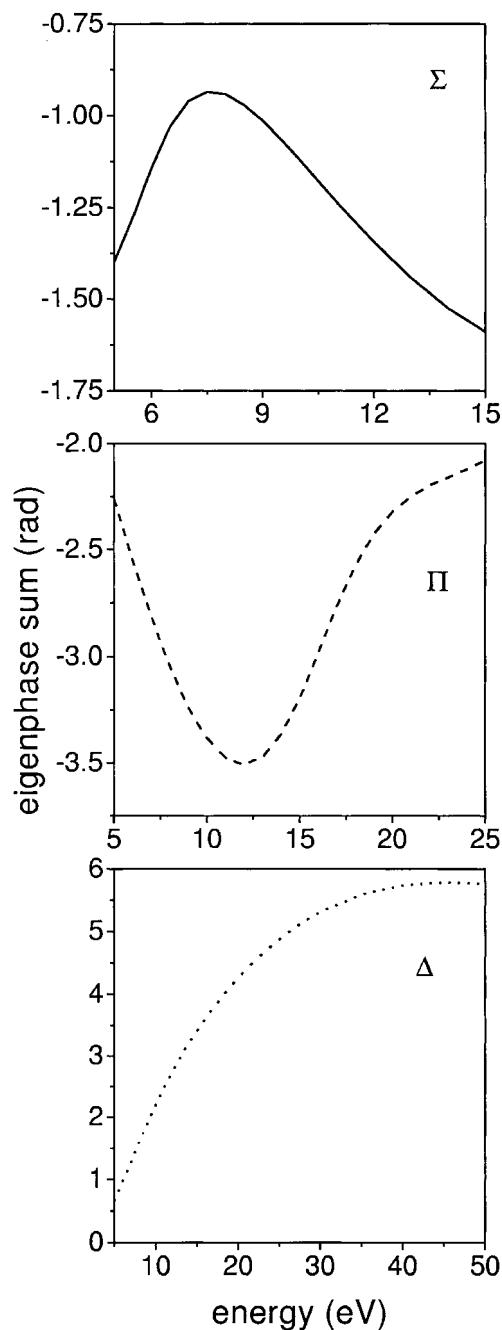| Type	O exponent	C exponent	S exponent	Coefficient
s	16·058780	12·496280	7·649093	1·0
s	5·920242	2·470286	1·743283	1·0
s	1·034907	0·614028	0·789128	1·0
s	0·316843	0·184028	0·302805	1·0
s	0·065203	0·039982	0·063479	1·0
p	10·141270	5·228869	7·203417	1·0
p	2·783023	1·592058	3·134723	1·0
p	0·841010	0·568612	0·529380	1·0
p	0·232940	0·210326	0·154155	1·0
p	0·052211	0·072250	0·035523	1·0
d	1·698024	1·794795	1·689035	1·0
d	0·455259	0·420257	0·476317	1·0
d	0·146894	0·101114	0·151558	1·0

Fig. 1.   Integral cross section for the OCS molecule: solid curve, our pseudopotentials results; dashed curve, theoretical results of Lynch and Dill (1979); crosses, experimental elastic data of Sohn *et al.* (1987); and stars, experimental total cross section of Szmytkowski *et al.* (1984).

$r(\text{C–O}) = 1 \cdot 1578$ Å and $r(\text{C–S}) = 1 \cdot 5601$ Å(CRC 1998). The 1s core electrons
of carbon and oxygen and the 1s, 2s and 2p core electrons of sulfur were replaced
by the pseudopotentials of Bachelet *et al.* (1982). The basis functions used in
the description of the target ground state $|\Phi_1\rangle$ and in the description of the
scattering orbitals $|\varphi_m\rangle$ used in equation (7) are given in Table 1, and were
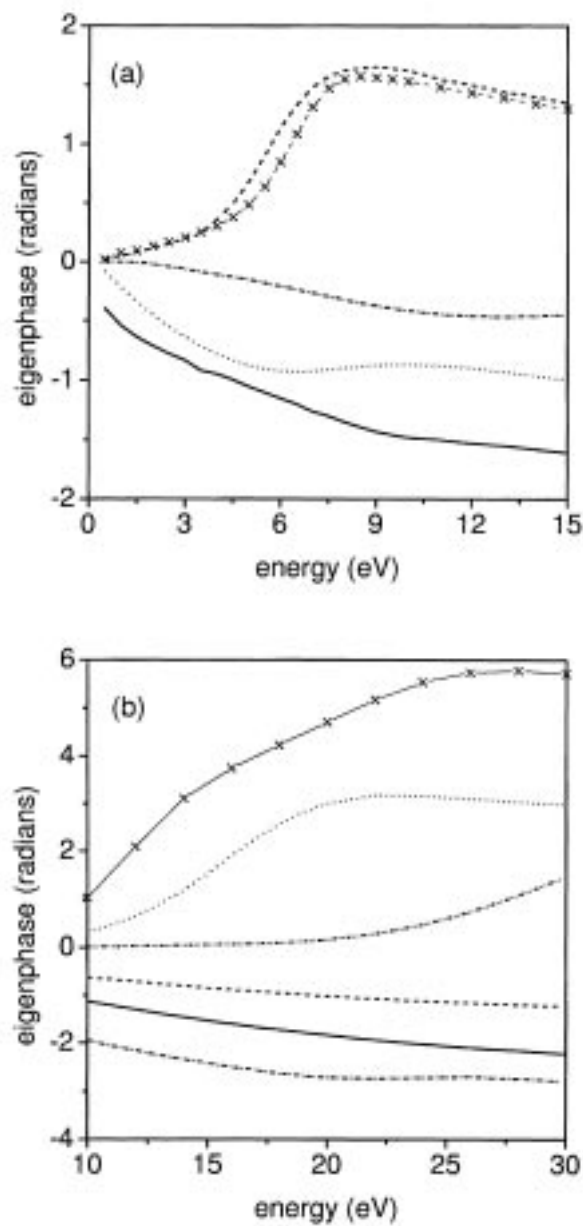

Fig. 2.   (*a*) Integral cross section for OCS and CS$_2$. (*b*) Symmetry decomposition of the
integral cross section for OCS (curves without crosses) and CS$_2$ (curves with crosses). The
symmetry decomposed cross sections of CS$_2$ are summed over the '*g*' and '*u*' labels.

obtained as described by Bettega *et al.* (1996). With this basis set, our calculated dipole moment is $0\cdot77\,\mathrm{D}$, which compares well with the experimental value of $0\cdot71\,\mathrm{D}$ (Szmytkowski *et al.* 1984). We have not included in our calculations the combination $\left[\left(x^2 + y^2 + z^2\right)\exp\left(-\alpha r^2\right)\right]$ in order to avoid linear dependency in the basis set, which could be responsible for spurious structures in the cross sections.

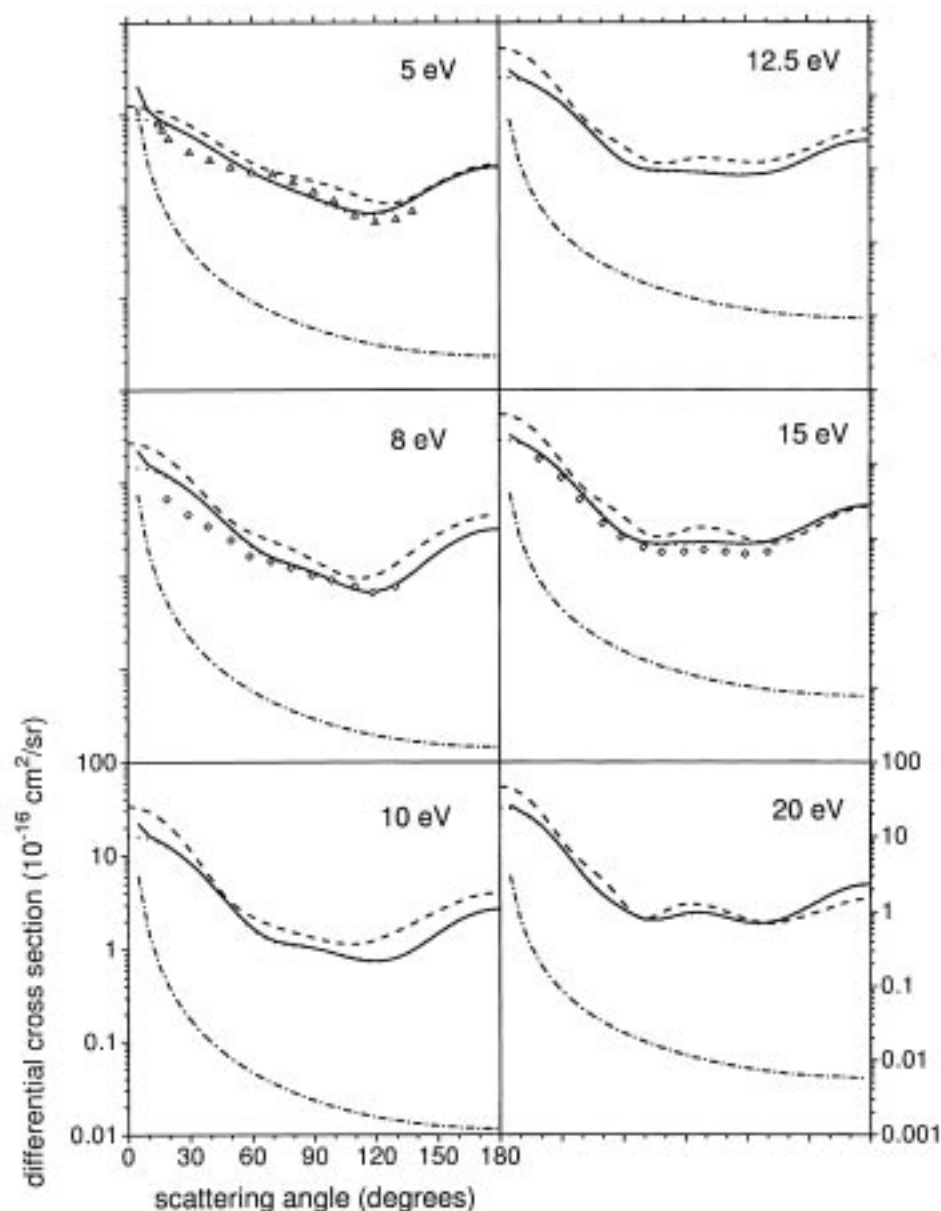**Fig. 3.** Eigenphase sum for the Σ, Π and Δ symmetries.

Fig. 4.   Eigenphases for (*a*) the Σ symmetry and (*b*) the Π symmetry. The curves with crosses are the related eigenphases for CS_2.
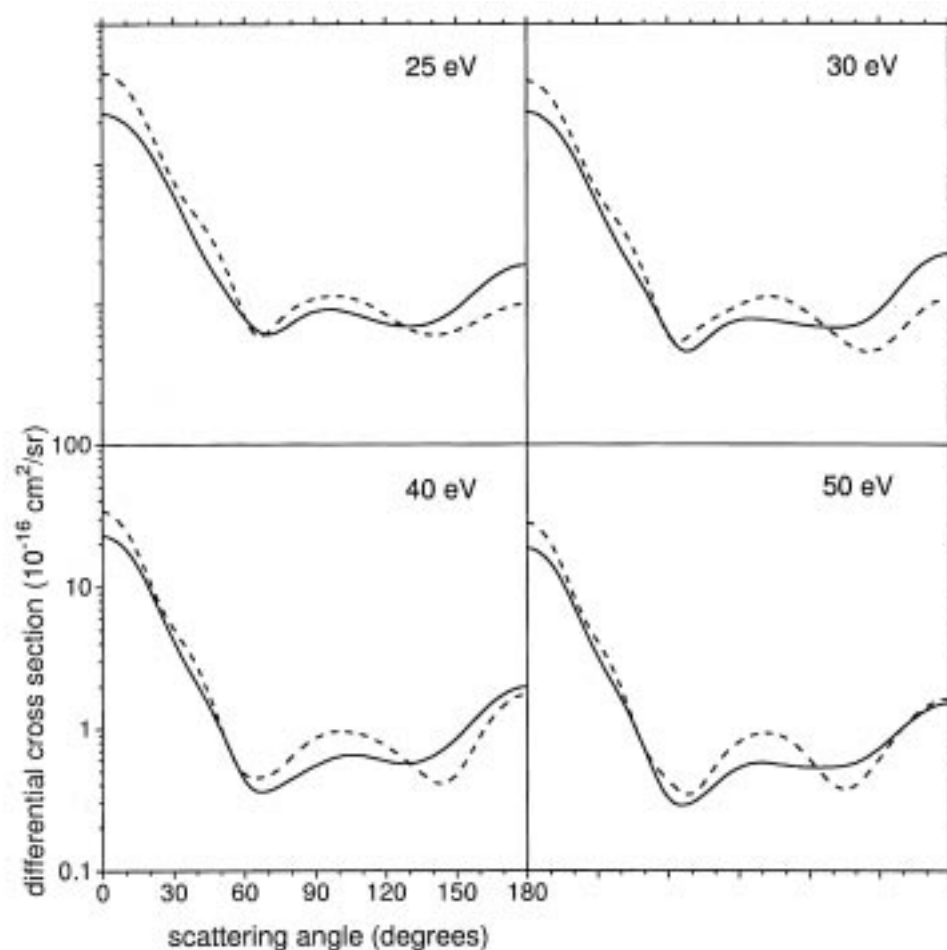
4. Results and Discussion

In Fig. 1 we compare our integral cross section (ICS) with the calculated cross section of Lynch and Dill (1979) and the measured total cross section of Szmytkowski *et al.* (1984). We also show the data at 5 eV of Sohn *et al.* (1987).

Fig. 5. Differential cross section for OCS at 5, 8, 10, 12·5, 15 and 20 eV: solid curve, SMCPP with Born; dotted curve, SMCPP without Born; dot–dash curve, dipole Born results; triangles, experimental elastic data of Sohn *et al.* (1987); and diamonds, experimental results of Sakamoto *et al.* (1999). The dashed curves are the differential cross sections of CS_2.

Our integral cross section presents two peaks, and as we will show below, they come from Σ and Π symmetries. The results of Lynch and Dill (1979) also present these two peaks, but they are shifted to lower energies compared to ours. Except for energies around 10 eV, the cross section of Lynch and Dill (1979) always lies above ours.

Fig. 6. As in Fig. 5, but for 25, 30, 40 and 50 eV. For these energies we have not included the FBA.

In Fig. 2a we compare our calculated ICS for OCS with our previous results for CS_2. Although the ICS of CS_2 is larger than that for OCS for the entire energy range considered, they show similar behaviour. In Fig. 2b we present the symmetry decomposition of the ICS for OCS and CS_2. For OCS, the decomposition shows that the two peaks, around 10 and 20 eV, come primarily from the Σ and Π symmetries respectively. In Lynch and Dill (1979) the first peak is a composition of Σ and Δ symmetries. In order to compare the symmetry decomposed cross sections of OCS and CS_2, we have summed the 'g' and 'u' cross sections of the same symmetry for CS_2. This procedure reflects the loss of the symmetry plane perpendicular to the molecular axis. A comparison is also shown in Fig. 2b. For each one of the symmetries, the cross section of CS_2 is always larger than that of OCS, but show the same features.

In order to identify possible shape resonances in the ICS of OCS we also calculated the eigenphase sum for the Σ, Δ and Π symmetries. The results
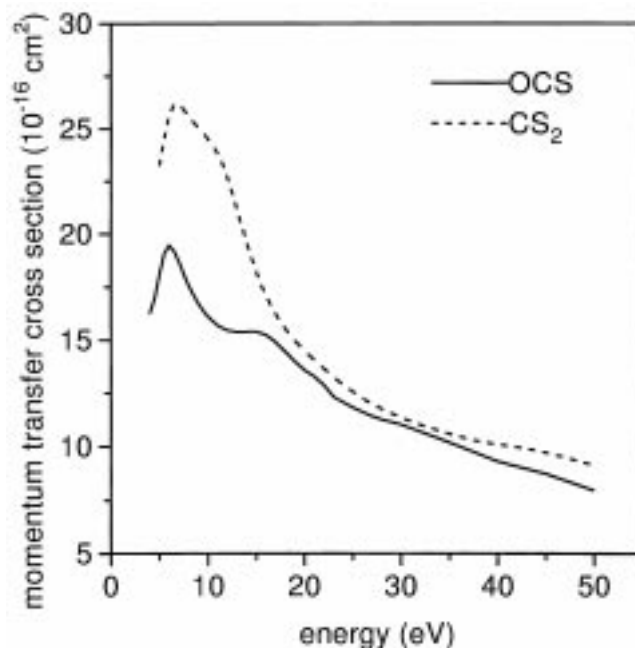
Fig. 7. Momentum tranfer cross sections for OCS and CS_2.

are shown in Fig. 3 and indicate that the peaks seen in Figs 1 and 2b may be interpreted as shape resonances. The symmetries shown in Fig. 2b have a background scattering and the eigenphase sum for each one of these symmetries has no need to exhibit the abrupt change of π (or even close to it) (Winstead and McKoy 1998). In order to illustrate this point, we show in Fig. 4 the eigenphases themselves (those which compose the eigenphase sum) for the overall Σ and Π symmetries of the OCS molecule. These eigenphases are obtained first through diagonalisation of the K-matrix and then by taking arctangents of the K-eigenvalues. It should be noted that some of these curves are strictly negative, while the resonant-like ones are positive. The eigenphase sum is fairly smooth but the eigenphase itself reveals a possible resonance. For comparison we have also included the related eigenphase of the Σ_g symmetry of CS_2 and the sum of the related eigenphases of the Π_g and Π_u symmetries of CS_2. The Δ resonance, being a very broad resonance, has a very short lifetime. Lynch and Dill (1979) also reported 'bumps' at the Σ and Δ symmetries around 5 eV. This behaviour is very similar to the CS_2 molecule (Bettega *et al.* 1999).

In Fig. 5 we present our differential cross section (DCS) at 5, 8, 10, 12·5, 15 and 20 eV. In each plot we show results obtained with the SMCPP method, with the SMCPP method combined with the FBA of the dipole moment potential, and the FBA of the dipole moment potential. At 5 eV we show the experimental results of Sohn *et al.* (1987); at 8 and 15 eV we also show the experimental results of Sakamoto *et al.* (1999). The agreement between theory and experiment is good. Following the plots one can see that the effect of the long range interaction due to the permanent dipole moment of OCS is just to correct the DCS at small

scattering angles and also that, as expected, as the energy becomes higher this correction becomes smaller. We also show our DCS for CS_2. Although the DCS of CS_2 are larger than the DCS of OCS, in general they are similar in shape. At 15 eV and at larger scattering angles, the DCS of OCS becomes larger than that for CS_2.

Fig. 6 shows the DCS at 25, 30, 40 and 50 eV, without including the FBA. At these energies there are no results available for comparison. As in Fig. 4, we also show our DCS for CS_2. At these energies the DCS of OCS is larger than that for CS_2 at higher scattering angles. Also, the DCS for these two molecules present two minima, around 60° and 150°. At 150° the minimum of CS_2 is more pronounced than the minimum of OCS. In Fig. 7 we compare the momentum transfer cross sections of OCS and CS_2. In Table 2 we present our results at selected energies.

Table 2.   Tabulated cross sections for OCS at selected energies

The cross sections are in units of 10^{-16} cm^2 and the scattering angles are in degrees. The differential cross sections from 5 to 20 eV include the Born correction

Angle (deg.)	5 eV	8 eV	10 eV	12·5 eV	15 eV	20 eV	25 eV	30 eV	40 eV	50 eV
0	—	—	—	—	—	—	23·15	23·71	22·89	18·64
5	20·83	22·50	22·22	22·46	24·65	26·36	22·23	22·61	21·61	17·49
10	11·38	16·00	16·72	17·64	19·90	21·74	19·70	19·62	18·24	14·49
20	7·98	11·88	12·40	12·80	13·68	13·98	12·29	11·37	9·62	7·27
30	6·09	8·33	8·37	8·12	7·90	7·10	5·99	5·19	4·19	3·21
40	4·49	5·35	5·02	4·47	4·00	3·18	2·73	2·44	2·07	1·62
50	3·25	3·30	2·82	2·29	2·00	1·66	1·40	1·27	0·98	0·70
60	2·41	2·13	1·69	1·32	1·16	1·07	0·80	0·62	0·43	0·32
70	1·87	1·58	1·26	1·01	0·89	0·80	0·61	0·46	0·36	0·30
80	1·51	1·32	1·13	0·96	0·86	0·81	0·72	0·63	0·44	0·40
90	1·24	1·10	1·03	0·94	0·89	0·95	0·89	0·76	0·55	0·53
100	1·03	0·88	0·90	0·89	0·89	0·97	0·90	0·77	0·64	0·57
110	0·88	0·72	0·79	0·85	0·87	0·84	0·81	0·73	0·64	0·55
120	0·84	0·68	0·75	0·84	0·85	0·72	0·72	0·70	0·59	0·53
130	0·96	0·82	0·82	0·88	0·90	0·72	0·69	0·68	0·57	0·53
140	1·26	1·18	1·05	1·05	1·11	0·86	0·74	0·70	0·64	0·57
150	1·70	1·76	1·49	1·40	1·50	1·17	0·93	0·89	0·86	0·73
160	2·18	2·43	2·04	1·89	2·05	1·66	1·29	1·37	1·27	1·02
170	2·56	2·99	2·51	2·33	2·58	2·14	1·70	1·99	1·76	1·36
180	2·70	3·20	2·70	2·51	2·80	2·35	1·89	2·29	1·98	1·52
ICS	27·68	30·68	29·46	28·46	28·50	26·63	23·21	21·33	18·05	14·53
MTCS	18·08	17·55	16·11	15·40	15·40	13·59	11·81	11·01	9·31	7·96

5. Summary

We have presented results for the elastic scattering of low-energy electrons by OCS molecules. Our results agree very well with the available theoretical and experimental results. Through the symmetry decomposition of the integral cross section and eigenphase sum analysis we found shape resonances for energies above 5 eV at the Σ, Π, and Δ symmetries. We have made a comparison between the results of OCS with our previous results for CS_2. These two molecules have the same number of valence electrons. We found a similar behaviour between the

symmetry decomposed cross sections of OCS and the 'g' and 'u' summed cross sections of CS_2, which reflects the loss of a symmetry plane by CS_2.

Acknowledgments

References

Bachelet, G., Hamann, D. R., and Schlüter, M. (1982). *Phys. Rev.* B **26**, 4199.
Bettega, M. H. F., Ferreira, L. G., and Lima, M. A. P. (1993). *Phys. Rev.* A **47**, 1111.
Bettega, M. H. F., Natalense, A. P. P., Lima, M. A. P., and Ferreira, L. G. (1996). *Int. J. Quant. Chem.* **60**, 821.
Bettega, M. H. F., Natalense, A. P. P., Lima, M. A. P., and Ferreira, L. G. (1999). Elastic scattering of low-energy electrons by carbon disulphide. *Braz. J. Phys.*, **30**, 184.
CRC (1998). 'CRC Handbook of Chemistry and Physics', 79th edn (Ed. D. R. Lide) (CRC Press: Boca Raton).
Lima, M. A. P., Brescansin, L. M., da Silva, A. J. R., Winstead, C., and McKoy, V. (1990). *Phys. Rev.* A **41**, 327.
Lynch, M. G., and Dill, D. (1979). *J. Chem. Phys.* **71**, 4249.
Raj, D., and Tomar, S. (1997). *J. Phys.* B **30**, 1989.
Sakamoto, Y., Watanabe, S., Hoshino, M., Okamoto, M., Kitajima, M., Tanaka, H., and Kimura, M. (1999). 'Progress Report on Atomic Collision Research in Japan', Vol. 25, p. 7 (Jap. Soc. for Atomic Collision Research).
Sohn, W., Kochem, K.-H., Scheuerlein, K. M., Jung, K., and Ehrhadt, H. (1987). *J. Phys.* B **20**, 3217.
Szmytkowski, C., Karwasz, G., and Maciag, K. (1984). *Chem. Phys. Lett.* **107**, 481.
Takatsuka, K., and McKoy, V. (1981). *Phys. Rev.* A **24**, 2473.
Takatsuka, K., and McKoy, V. (1984). *Phys. Rev.* A **30**, 1734.
Varella, M. T. do N., Bettega, M. H. F., da Silva, A. J. R., and Lima, M. A. P. (1999). *J. Chem. Phys.* **110**, 2452.
Winstead, C., and McKoy, V. (1998). *Phys. Rev.* A **57** , 3589.